

Supporting Information for

Structure and Electrochemical Properties of $\text{Na}_{2\pm x}\text{V}_3\text{P}_2\text{O}_{13}$ ($x = 0$ and 1): A Promising Cathode Material for Sodium-Ion Batteries

M. Anji Reddy ^{a,*}, Holger Euchner ^a, Raiker Wetter ^{b,d}, and Oliver Clemens ^{c,d}

^a Helmholtz Institute Ulm (HIU) for Electrochemical Energy storage, Helmholtz Str.11, 89081 Ulm, Germany

^b School of Information Technologies, Tallinn University of Technology, Ehitajate tee 5, 19086 Tallinn, Estonia.

^c Technische Universität Darmstadt, Institut für Materialwissenschaft, Fachgebiet Materialdesign durch Synthese, Alarich-Weiss-Straße 2, 64287 Darmstadt, Germany.

^d Karlsruher Institut für Technologie, Institut für Nanotechnologie, Hermann-von-Helmholtz-Platz 1, 76344 Eggenstein-Leopoldshafen, Germany.

*Corresponding author Email: munnangi.reddy@kit.edu

Table S1. Comparison of state-of-the-art cathode materials for NIBs

NIB cathode materials	Ave. Potential (V) vs. Na/Na ⁺	Sp. Capacity (mAh g ⁻¹)	Sp. Energy (Wh kg ⁻¹)
O3-NaMn _{0.25} Fe _{0.5} Ni _{0.25} O ₂	3.0	140	420
P2- Na _x Mg _{0.11} Mn _{0.89} O ₂	3.0	148	444
P3/P2/O3-Na _{0.76} Mn _{0.5} Ni _{0.3} Fe _{0.1} Mg _{0.1} O ₂	3.3	155	511
Na ₂ Fe(PO ₄)F	3.0	100-124	300-372
Na ₃ V ₂ (PO ₄) ₃	3.4	117	397
Na ₃ V ₂ (PO ₄) ₂ F ₃	3.9	120	468
Na ₂ Fe ₂ (SO ₄) ₃	3.8	100-120	380-456

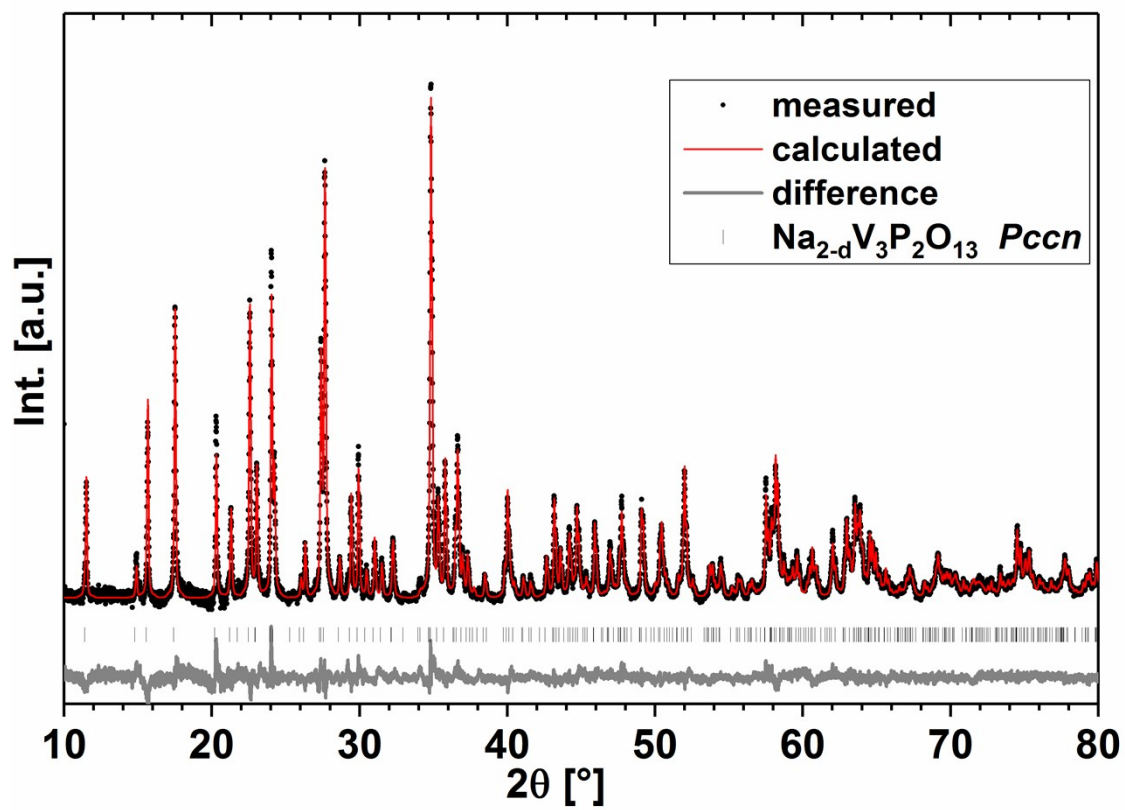


Figure S1. Rietveld analysis of powder XRD patterns recorded for $\text{Na}_{2-x}\text{V}_3\text{P}_2\text{O}_{13}$

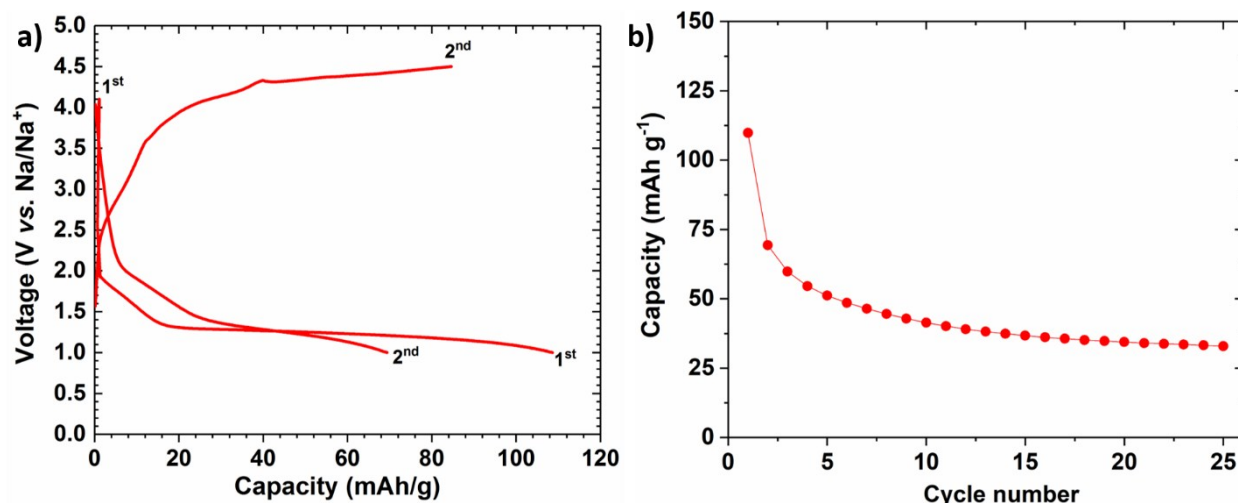


Figure S2 a) discharge and charge curves of as synthesized $\text{Na}_2\text{V}_3\text{P}_2\text{O}_{13}$ for the first two cycles, b) cycling behaviour of the same cell. The discharge-charge curves were obtained at 25 °C, at a current rate of C/20 and in the voltage window of 1.0-4.5 V vs. Na/Na⁺. Capacities were calculated based on the weight of the active material.

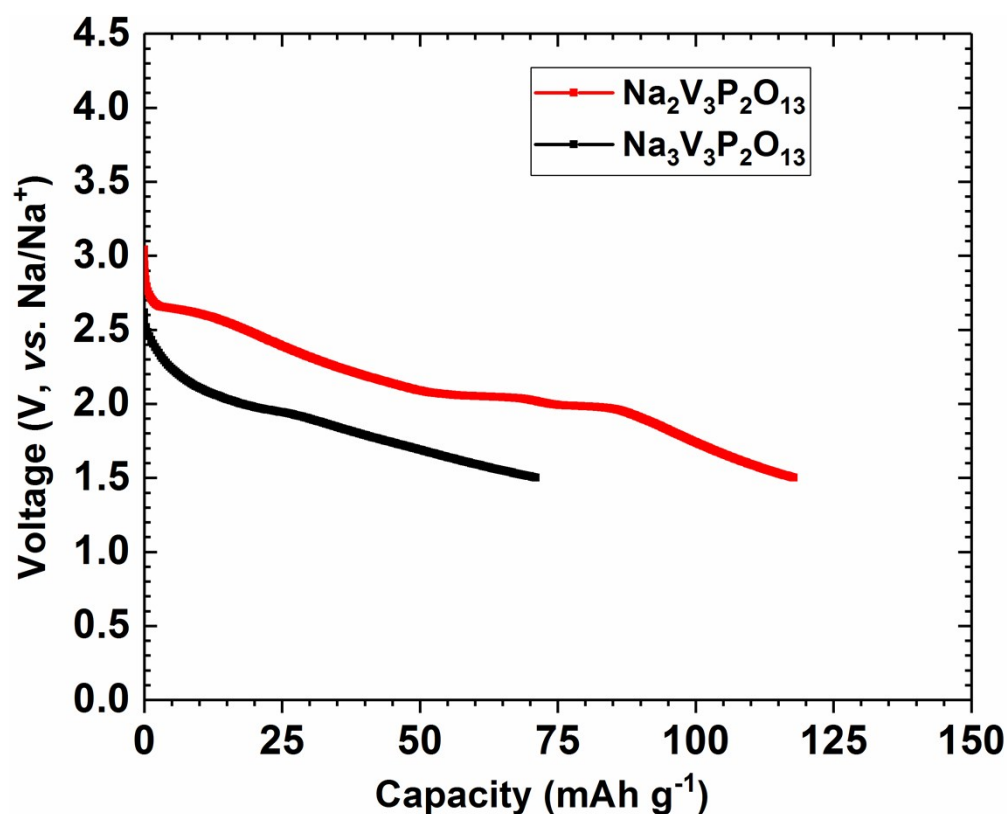


Figure S3 first discharge curves of $\text{Na}_2\text{V}_3\text{P}_2\text{O}_{13}$ and $\text{Na}_3\text{V}_3\text{P}_2\text{O}_{13}$. The discharge curves were obtained at 25 °C, at a current rate of C/20 and the cells were discharged to 1.5 V vs. Na/Na⁺. Capacities were calculated based on the weight of the active material.

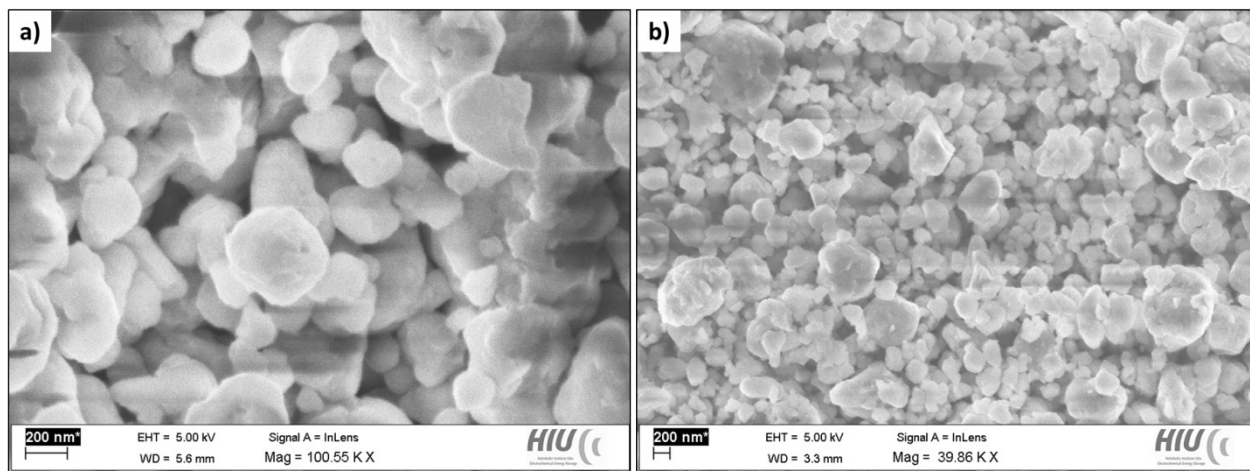


Figure S4 SEM images of a) $\text{Na}_2\text{V}_3\text{P}_2\text{O}_{13}$ and b) $\text{Na}_3\text{V}_3\text{P}_2\text{O}_{13}$

Table S2. Structural data of $\text{Na}_2\text{V}_3\text{P}_2\text{O}_{13}$ determined from Rietveld analysis of X-ray powder diffraction data. Oxidation states of the different vanadium ions are assigned according to determination of bond distances in agreement with DFT based calculations reported in section 0.

Wyckoff site / site label	atom type	x	y	z	occ.	B [\AA^2]
<i>8e / Na1</i>	Na^+	0.2155(4)	0.0464(3)	0.1075(4)	1	0.50(3)
<i>8e / V1</i>	V^{5+}	0.4796(2)	0.3676(2)	0.7555(3)	1	0.50(3)
<i>4d / V2</i>	V^{4+}	$1/4$	$3/4$	0.5624(4)	1	0.50(3)
<i>8e / P1</i>	P^{5+}	0.4849(3)	0.1249(5)	0.8715(3)	1	0.50(3)
<i>8e / O1</i>	O^{2-}	0.4288(6)	0.5037(5)	0.3046(8)	1	0.50(3)
<i>8e / O2</i>	O^{2-}	0.4216(5)	0.1450(4)	0.0469(7)	1	0.50(3)
<i>8e / O3</i>	O^{2-}	0.3513(5)	0.0862(5)	0.3544(7)	1	0.50(3)
<i>8e / O4</i>	O^{2-}	0.8682(5)	0.1160(5)	0.3921(6)	1	0.50(3)
<i>8e / O5</i>	O^{2-}	0.5903(5)	0.1489(5)	0.3940(7)	1	0.50(3)
<i>8e / O6</i>	O^{2-}	0.0635(5)	0.2093(5)	0.2437(7)	1	0.50(3)
<i>4d / O7</i>	O^{2-}	$1/4$	$3/4$	0.8672(10)	1	0.50(3)
a [\AA]	10.1096(1)	b [\AA]	11.9790(1)	c [\AA]	8.3842(1)	
R_{wp}	8.3 %	R_{Bragg}	3.3 %	GOF	1.12	

Table S3. Structural data of chemically sodiated $\text{Na}_3\text{V}_3\text{P}_2\text{O}_{13}$ determined from Rietveld analysis of X-ray powder diffraction data. Oxidation states of the different vanadium ions are assigned according to determination of bond distances in agreement with DFT based calculations reported in section 0.

Wyckoff site / site label	atom type	x	y	z	occ.	B [\AA^2]
<i>8e / Na1</i>	Na^+	0.2245(4)	0.0050(4)	0.0723(7)	1	1.00(5)
<i>4c / Na2</i>	Na^+	$1/4$	$1/4$	0.5243(8)	1	1.00(5)
<i>8e / V1</i>	V^{4+}	0.4786(2)	0.3705(2)	0.7507(4)	1	1.00(5)
<i>4d / V2</i>	V^{5+}	$1/4$	$3/4$	0.6491(5)	1	1.00(5)
<i>8e / P1</i>	P^{5+}	0.4806(3)	0.1205(3)	0.8514(4)	1	1.00(5)
<i>8e / O1</i>	O^{2-}	0.4404(5)	0.4956(6)	0.2662(11)	1	1.00(5)
<i>8e / O2</i>	O^{2-}	0.4182(5)	0.1302(5)	0.0403(9)	1	1.00(5)
<i>8e / O3</i>	O^{2-}	0.3557(6)	0.1049(6)	0.3580(10)	1	1.00(5)
<i>8e / O4</i>	O^{2-}	0.8759(6)	0.1210(6)	0.3659(9)	1	1.00(5)
<i>8e / O5</i>	O^{2-}	0.6199(6)	0.1653(5)	0.3705(10)	1	1.00(5)
<i>8e / O6</i>	O^{2-}	0.0621(6)	0.2029(5)	0.2320(10)	1	1.00(5)
<i>4d / O7</i>	O^{2-}	$1/4$	$3/4$	0.8436(16)	1	1.00(5)
a [\AA]	10.3095(4)	b [\AA]	12.5169(4)	c [\AA]	8.0943(3)	
R_{wp}	3.2 %	R_{Bragg}	0.9 %	GOF	1.33	

Table S4. Structural data of chemically prepared $\text{Na}_{2-x}\text{V}_3\text{P}_2\text{O}_{13}$ determined from Rietveld analysis of X-ray powder diffraction data. Refinement of the Na site occupation did not prove to be stable and was therefore fixed to a value determined independently.

Wyckoff site / site label	atom type	x	y	z	occ.	B [\AA^2]
<i>8e / Na1</i>	Na^+	0.2145(3)	0.0466(2)	0.1040(3)	0.908(4)	1.19(3)
<i>8e / V1</i>	V^{5+}	0.4801(1)	0.3669(1)	0.7556(2)	1	1.19(3)
<i>4d / V2</i>	V^{5+}	$1/4$	$3/4$	0.5616(2)	1	1.19(3)
<i>8e / P1</i>	P^{5+}	0.4878(2)	0.1203(2)	0.8720(2)	1	1.19(3)
<i>8e / O1</i>	O^{2-}	0.4363(3)	0.5009(3)	0.2980(5)	1	1.19(3)
<i>8e / O2</i>	O^{2-}	0.4215(3)	0.1417(3)	0.0453(5)	1	1.19(3)
<i>8e / O3</i>	O^{2-}	0.3513(4)	0.0870(3)	0.3481(5)	1	1.19(3)
<i>8e / O4</i>	O^{2-}	0.8671(3)	0.1216(3)	0.3886(4)	1	1.19(3)
<i>8e / O5</i>	O^{2-}	0.5919(3)	0.1499(3)	0.3802(4)	1	1.19(3)
<i>8e / O6</i>	O^{2-}	0.0593(3)	0.2049(3)	0.2456(5)	1	1.19(3)
<i>4d / O7</i>	O^{2-}	$1/4$	$3/4$	0.8807(6)	1	0.50(3)
a [\AA]	10.1882(2)	b [\AA]	11.9785(3)	c [\AA]	8.3832(2)	
R_{wp}	3.5 %	R_{Bragg}	1.7 %	GOF	1.50	

Table S5. Refined bond distances of $\text{Na}_2\text{V}_3\text{P}_2\text{O}_{13}$ together with most likely assignment of vanadium oxidation states in agreement with DFT based calculations and bond distances which would be expected from Shannon's ionic radii.

d(Na1-Ox) [Å]		d(V1-Ox) [Å] (8e site)		d(V2-Ox) [Å] (4d site)		d(P1-Ox) [Å]	
O3	2.274(7)	O5	1.625(6)	O7	1.637(9)	O4	1.499(6)
O1	2.288(7)	O3	1.636(6)	O4	2.037(6)	O7	1.552(7)
O2	2.448(7)	O2	1.851(6)	O4	2.037(6)	O2	1.622(7)
O4	2.484(7)	O1	1.868(6)	O5	2.051(5)	O1	1.735(7)
O3	2.533(7)	O6	1.948(7)	O5	2.051(5)		
O5	2.660(7)			O7	2.555(9)		
O6	2.736(7)						
O1	3.382(8)						
d _{mean}	2.60	d _{mean}	1.79	d _{mean}	1.96 (CN=5) 2.06 (CN=6)	d _{mean}	1.60

Table S6. Refined bond distances of chemically sodiated $\text{Na}_3\text{V}_3\text{P}_2\text{O}_{13}$ together with most likely assignment of vanadium oxidation states in agreement with DFT based calculations and bond distances which would be expected from Shannon's ionic radii¹³.

d(Na1-Ox) [Å]		d(Na2-Ox) [Å]		d(V1-Ox) [Å] (8e site)		d(V2-Ox) [Å] (4d site)		d(P1-Ox) [Å]	
O4	2.274(8)	O2	2.296(6)	O3	1.567(7)	O7	1.574(14)	O6	1.481(8)
O3	2.293(9)	O2	2.296(6)	O5	1.806(7)	O5	1.717(6)	O4	1.484(7)
O1	2.314(9)	O3	2.510(8)	O2	1.813(8)	O5	1.717(6)	O1	1.661(8)
O5	2.433(7)	O3	2.510(8)	O1	1.878(8)	O4	2.075(7)	O2	1.663(8)
O2	2.551(7)	O6	2.631(9)	O6	2.145(7)	O4	2.075(7)		
O3	2.957(9)	O6	2.631(9)			O7	2.473(14)		
O6	3.257(8)	O6	3.114(9)						
O1	3.331(9)	O6	3.114(9)						
		O3	3.433(9)						
		O3	3.433(9)						
d _{mean}	2.68	d _{mean}	2.64	d _{mean}	1.84	d _{mean}	1.83 (CN=5) 1.94 (CN=6)	d _{mean}	1.57

Table S7. Lattice parameters obtained from DFT calculations on $\text{Na}_y\text{V}_3\text{P}_2\text{O}_{13}$ ($y = 1-3$).

compound	symmetry	a [Å]	b [Å]	c [Å]
$\text{Na}_1\text{V}_3\text{P}_2\text{O}_{13}$	$Pc2_1n$	10.250	12.103	8.439
$\text{Na}_2\text{V}_3\text{P}_2\text{O}_{13}$	$Pccn$	10.345	12.155	8.420
$\text{Na}_3\text{V}_3\text{P}_2\text{O}_{13}$	$Pccn$	10.4584	12.6304	8.111

Table S8. Calculated bond distances for DFT calculated structure optimizations of $\text{Na}_y\text{V}_3\text{P}_2\text{O}_{13}$ ($y = 1-3$). * := For $\text{Na}_1\text{V}_3\text{P}_2\text{O}_{13}$ bond distances as obtained for the ordering of sodium ions belonging to a lowering of symmetry are given exemplarily ($Pccn \rightarrow Pc2_1n$), resulting in a splitting of the 8e site to two sites with 4-fold multiplicity.

d(V1-O) [Å] (8e site)				d(V2-O) [Å] (4d site)		
$\text{Na}_1\text{V}_3\text{P}_2\text{O}_{13}^*$ (V^{5+})		$\text{Na}_2\text{V}_3\text{P}_2\text{O}_{13}$ (V^{5+})	$\text{Na}_3\text{V}_3\text{P}_2\text{O}_{13}$ (V^{4+})	$\text{Na}_1\text{V}_3\text{P}_2\text{O}_{13}^*$ (V^{5+})	$\text{Na}_2\text{V}_3\text{P}_2\text{O}_{13}$ (V^{4+})	$\text{Na}_3\text{V}_3\text{P}_2\text{O}_{13}$ (V^{5+})
1.635	1.602	1.628	1.649	1.626	1.622	1.634
1.748	1.810	1.764	1.753	1.837	1.868	1.877
1.910	1.884	1.940	1.956	1.864	1.868	1.877
1.942	1.931	1.960	2.012	1.902	1.999	2.039
1.944	1.990	1.985	2.081	1.968	1.999	2.039
				2.595	2.588	2.422
d_{mean}						
1.84	1.84	1.855	1.89	1.84 (CN=5) 1.97 (CN=6)	1.87 (CN=5) 1.99 (CN=6)	1.89 (CN=5) 1.98 (CN=6)

Table S9. Calculated voltages for sodium insertion and extraction steps of $\text{Na}_2\text{V}_3\text{P}_2\text{O}_{13}$. * := different distributions of sodium ions on the 8e site were investigated, resulting in slightly different energies.

Reaction of respective cycling step	Theoretical voltage against metallic sodium [V]
$\text{Na}_3\text{V}_3\text{P}_2\text{O}_{13} \rightarrow \text{Na}_2\text{V}_3\text{P}_2\text{O}_{13} + \text{Na}^+ + \text{e}^-$	1.97
$\text{Na}_2\text{V}_3\text{P}_2\text{O}_{13} \rightarrow \text{Na}_1\text{V}_3\text{P}_2\text{O}_{13} + \text{Na}^+ + \text{e}^-$	3.23 - 3.29*